Faculty Publications   Electrical Engineering, Department of

Low Cost Schottky Barrier Solar Cells Fabricated on CdSe and Sb$_2$S$_3$ Films Chemically Deposited with Silicotungstic Acid

O. Savadogo

K. C. Mandal
University of South Carolina - Columbia, mandalk@engr.sc.edu

Follow this and additional works at: https://scholarcommons.sc.edu/elct_facpub

Part of the Electrical and Electronics Commons, Other Chemical Engineering Commons, and the Other Electrical and Computer Engineering Commons

protons, coupled with the high mobility of hydrogen or protons in oxides.[4]

Conclusion

Amorphous electrochromic niobium oxide thin films can be prepared by CVD at 350°C using niobium(V) ethoxide as a source material. Reduction and oxidation of these films in a $0.1M$ Na_2CO_3 + $0.1M$ $NaHCO_3$ buffer solution resulted in desirable changes in optical absorption. Coulometry experiments indicated that the coloration efficiency of the amorphous film was 160 $cm^2 \cdot C^{-1}$ which is much higher than for the film prepared by a radio-frequency magnetron sputtering method suggesting that low temperature CVD offers an attractive way of preparing electrochromic Nb_2O_5 films.

Acknowledgment

REFERENCES

1. C. K. Dyer and J. S. L. Leach, *This Journal,* **125,** 23 (1978).
2. B. Reichman and A. J. Bard, *ibid.,* **127,** 241 (1980).
3. M. A. B. Gomes, L. O. S. Bulhões, S. C. Castro, and A. J. Damião, *ibid.,* **137,** 3068 (1990).
4. T. Maruyama and S. Arai, *Appl. Phys. Lett.,* **63,** 869 (1993).
5. M. Duffy, C. C. Wang, A. Waxman, and K. H. Zaininger, *This Journal,* **116,** 234 (1969).
6. J. C. Manifacier, J. Gasiot, and J. P. Fillard, *J. Phys. E.,* **9,** 1002 (1976).
7. P. C. Karulkar and J. E. Nordman, *J. Vac. Sci. Technol.,* **17,** 462 (1980).
8. C. K. Dyer and J. S. L. Leach, *Electrochim. Acta,* **20,** 151 (1975).

Low Cost Schottky Barrier Solar Cells Fabricated on CdSe and Sb₂S₃ Films Chemically Deposited with Silicotungstic Acid

O. Savadogo* and K. C. Mandal

Département de Métallurgie et de Génie des Matériaux, École Polytechnique de Montréal, Montréal, Québec, Canada H3C 3A7

ABSTRACT

A novel method for fabricating high efficiency metal (Pt, Au, and Ni)/(CdSe or Sb_2S_3) Schottky barrier solar cells is reported. The method is based on the fabrication of n-CdSe or Sb_2S_3 thin films chemically deposited with and without silicotungstic acid (STA). The performances of the Schottky junctions fabricated with the films deposited with STA, CdSe(STA), or Sb_2S_3(STA), are significantly higher than those deposited without STA. Under AM1 illumination, the photovoltaic properties of the improved Pt/CdSe(STA) diode showed V_{oc} = 0.72 V, J_{sc} = 14.1 mA/cm², $FF \simeq$ 0.70, and efficiency $\eta \simeq$ 7.2%. Analogous results are obtained on Pt/n-Sb_2S_3(STA), where the photovoltaic response of the improved diode showed V_{oc} = 0.63 V, J_{sc} = 11.3 mA/cm², $FF \simeq$ 0.63, and $\eta \simeq$ 5.5%. The ideality factor (n) and saturation current density (J_0) were also significantly improved. C-V measurements at 1 MHz showed that the barrier height (ϕ_b) of the fabricated diodes are 0.62 and 0.59 eV for Pt/CdSe and Pt-Sb_2S_3 junctions, respectively, and 0.81 and 0.80 eV for Pt/CdSe(STA) and Pt-Sb_2S_3(STA) junctions, respectively. It is also observed that the ϕ_b values are independent of the metal work functions (W). This is attributed to the Fermi level pinning of CdSe or Sb_2S_3 films deposited with and without STA.

The diode ideality factor (n) and the saturation current density (J_0) are probably the most important parameters in Schottky diode solar cells. The classical relationship of the J-V characteristics of the diodes is given by

$$J = J_0 \left[\exp\left(\frac{qV}{nkT}\right) - 1 \right] \qquad [1]$$

where n is the diode ideality factor. For an ideal Schottky barrier, n equals 1, and the dark saturation current density J_0 is given by

$$J_0 = A^{**}T^2 \exp\left(-q\phi_b/kT\right) \qquad [2]$$

where A^{**} is the Richardson constant and ϕ_b is the barrier height which depends on the bandgap (E_g), the electron affinity (χ) of the semiconductor, the metal work function (Wm), and the diode interface state density and distribution. Furthermore, for a given semiconductor, the variation of ϕ_b with Wm may indicate interface behavior due to the presence of interface states. Consequently, modification of the semiconductor may give information on the change in barrier height. Considerable effort has been expended recently in trying to understand the properties of the Schottky barrier height ϕ_b in an attempt to increase the open-circuit voltage V_{oc} of solar cells.

* Electrochemical Society Active Member.

The development of high efficiency Schottky barrier solar cells based on thin-film semiconductor is limited because of the relatively poor characteristics observed up to now. One recent approach for overcoming this problem is based on the growth of thin passivating surface layers on top of an active layer. This layer may be an insulator or a layer of a higher bandgap semiconductor.[1] The increase in the effective barrier height occurs due to the bandgap discontinuity at the interface between an active layer and a surface layer. Recently, it has been observed that Schottky barrier heights on n-CdTe can be enhanced from ϕ_b = 0.67 to 0.92 eV by incorporating a thin insulating layer.[2] Surface modification by metallic ion adsorption (*e.g.*, Zn^{2+}) or by forming high insulating $[Cd(CN)Fe(CN)_6]^{2-/1-}$ layers are very useful for improving the performance of n-CdSe based photoelectrochemical (PEC) solar cells,[3–6] which are in many ways similar to Schottky barriers. Another possibility was to obtain an enhanced barrier height by creating additional band bending, which is produced by the chemical adsorption of metals and their successive oxidation, for growing very thin metal oxide layers on top of the substrates. This results in an increase in barrier height[7] from 0.5 to 0.73 eV on silicon. Unfortunately, the fabricated diode exhibited high reverse saturation current densities (J_0) and nonideal behavior in the forward bias region.

Among the metal sulfides, antimony trisulfide is particularly well-suited to use as a target material for TV cameras,[8] microwave devices,[9] switching devices,[10] and various optoelectronic devices.[11-13] The films were prepared by a vacuum evaporation technique using powdered Sb_2S_3 compounds as the starting material. This causes some departures in the stoichiometry of the deposited film which are mainly due to large differences in the vapor pressures of the constituents at the deposition temperature. CdSe is a promising semiconductor material for solar cells and various optoelectronic devices, with a bandgap of 1.7 eV. Photoelectrochemical (PEC) solar cells with single-crystal n-CdSe photoanodes have been studied[14,15] and an efficiency of 7 to 8% obtained. It has been indicated that with appropriate electrolyte modification, the PEC efficiency of n-CdSe single crystals can be improved (~16%).[16] Moreover, the high cost of single-crystal electrodes, which is one of the most limiting factors for their large-area fabrication, can be avoided easily by replacing the electrodes with polycrystalline films or pellets. On the other hand, the high cost of single-crystal electrodes, remains a seriously limiting factor in the fabrication of metal/CdSe solar cells. Using polycrystalline films is an interesting approach, however, and as a result there has been considerable interest in developing new polycrystalline thin film semiconductors, such as Sb_2S_3 or CdSe.[17-20] These polycrystalline films may be prepared by many methods, such as electrodeposition,[21] vacuum evaporation,[22] screen printing,[23] spray pyrolysis,[24] and pressure sintering.[25] Among them, chemical deposition deserves special attention because it has been to be an inexpensive, low temperature, and nonpolluting method. Moreover, the quality of the films in terms of the electrical and optical properties can be altered easily by incorporating suitable species in the chemical bath. Thus, sophisticated technologies, such as photolithography, diffusion, ion implantation, etc., are not required to create a material with the desired properties. The method is also very suitable for making large area films of any configuration. In previous work,[26-30] we have introduced new chemical methods for the deposition of CdSe and Sb_2S_3 thin films and demonstrated that there is significant improvement in their photovoltaic properties when silicotungstic acid is used in the deposition bath. An improved Au/n-Sb_2S_3 Schottky diode on the n-Sb_2S_3 films deposited with STA ($n = 1.08, J_0 = 1.5 \times 10^{-9}$ A/cm²) with a barrier height enhanced up to 0.76 eV has been described in our previous communication.[28] Recently, we have reported the first fabrication of low cost n-Sb_2S_3/p-Si and n-Sb_2S_3/p-Ge heterojunction solar cells using the chemical deposition method.[29,30]

This present communication describes for the first time a novel and simple approach on the photovoltaic properties of metal (Pt, Au, and Ni)/(n-CdSe or n-Sb_2S_3) Schottky barriers fabricated with n-CdSe or Sb_2S_3 films deposited with and without STA. In particular, the significant improvement in the junction properties for films deposited with STA has been described and the behavior of the barrier height of the junctions for different metal work functions has been studied.

Experimental

The Schottky barrier structures were fabricated on low cost chemically deposited polycrystalline n-CdSe and n-Sb_2S_3 films on ITO coated glass. The films deposited with STA are designated CdSe(STA) and Sb_2S_3(STA) and those deposited without STA are designated CdSe and Sb_2S_3. The film preparation methods have been reported previously.[26,27] The basic part of the structure consisted of an ITO-coated layer ($R_\square = 1.5$-2.0 Ω). Over it, a 5.2 μm n-CdSe or 3.8 μm n-Sb_2S_3 layer was grown chemically from four successive fresh chemical deposition baths. The resulting films were thermally annealed at 650 K for 1 h in an N_2-ambient atmosphere. Prior to metal deposition, the n-CdSe and n-Sb_2S_3 films were etched in 2% HCl for 5 to 10 s and dried in purified nitrogen. Pt, Ni, and Au of 6N purity was evaporated in a vacuum of 10^{-6} Torr, and the diodes with different areas in the 0.04 to 0.09 cm² range were prepared

using a proper masking arrangement so as to form a circular device. The Schottky structures were then annealed at 400 K for 5 min in an H_2 atmosphere to improve the reproducibility of the results. The semitransparent metal films (125 ± 5 Å) served as the rectifying contact, while the ITO-backed contact on the CdSe or Sb_2S_3 films acted as the ohmic contact. Voltage and current were controlled by a Princeton Applied Research (PAR) Model 273A potentiostat/galvanostat, and traces were recorded on a BBC Goerz Metrawatt Instruments recorder, Model SE 790 X-Y. A 300 W tungsten-halogen light (Fiber-Lite 180) was used, the intensities of which were calibrated by an Oriel solar simulator radiometer (Model 81020). The light was incident from the semitransparent metal film side. Several current measurements were taken for each voltage step to improve the signal-to-noise ratio in the very low current regime. The capacitance measurements as a function of applied voltage (C-V) at 1 MHz were taken using a Schlumberger SI 1255 HF response analyzer with a Solartron 1286 electrochemical interface. The experiments were controlled by an Altech microcomputer via an IEEE 488 bus.

Results and Discussion

Structural, electrical, and optical properties.—The n-CdSe and n-Sb_2S_3 films were characterized through resistivity, Hall effect measurements, x-ray diffraction (XRD), neutron activation analysis (NAA), x-ray photoelectron spectroscopy (XPS), and optical absorption measurements as described in our earlier publications.[26-31] The NAA and XPS analysis show the presence of WO_3 (triclinic phase) in the CdSe and Sb_2S_3 films deposited with STA.[26-30] The resistivity and carrier concentration measurements were carried out by the classical Hall effect technique on CdSe and Sb_2S_3 films deposited with and without STA and are summarized in Table I. As may be seen, the films deposited with and without STA have approximately the same resistivity, carrier concentration, and carrier mobility. On the other hand, it may be seen from Fig. 1 and 2 that the optical absorption $(\alpha h v)^2$ *vs.* incident photon energy (hv) curves change for CdSe and Sb_2S_3 films deposited with and without STA. An identical ITO-coated glass substrate was used as the reference and the values of the optical absorption coefficient (α) were not corrected for the reflectance of the film surface. The values of the optical bandgap (E_g) do not change significantly for films deposited with and without STA. However, for both CdSe and Sb_2S_3 films, the optical absorption coefficients of electrodes deposited with STA (α_1) are higher than those of films deposited without STA (α_2).

Solar cell properties.—The dark I-V characteristics of the Pt/n-CdSe(STA) and 0.09 cm² Pt/n-CdSe Schottky diode were measured at room temperature (300 K). Nearly the same characteristics were obtained on structures 0.06 and 0.08 cm² in area. The ideality factor n, barrier height ϕ_b, and reverse saturation current density (J_0) were used to characterize the properties of the fabricated devices and to compare the effects of STA. The good quality of these Schottky diodes may be seen from Fig. 3. They follow the linear relationship of the ln (J)-V plot over at least four orders of current, and they have very low reverse current densities: $J_0 = 1.3 \times 10^{-9}$ A/cm² for Pt/CdSe(STA) and $J_0 = 3.8 \times 10^{-7}$ A/cm² for Pt/CdSe. The ideality factor is close to unity (*e.g.*, 1.04) for the Pt/CdSe(STA) film, whereas a higher value of n (*e.g.*, 1.84) is obtained for the Pt/CdSe.

Table I. Resistivity ρ, carrier concentration (N_d) and mobility (μ_n) of the n-CdSe and n-Sb_2S_3 films deposited with and without STA and annealed at 430°C.

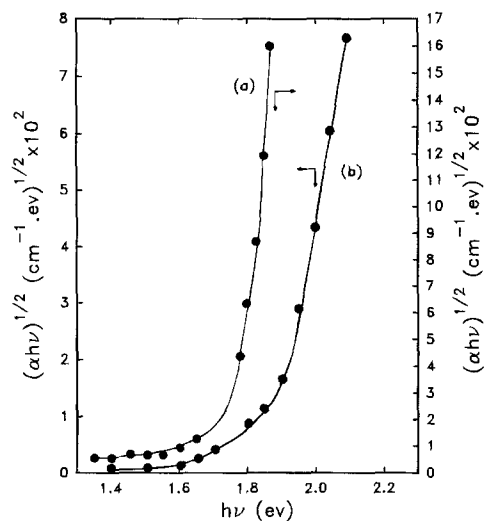| Films	Resistivity (ρ) (Ω · cm)	Carrier concentration (N_d) (cm⁻³)	Mobility (μ_n) (cm²/V-s)
CdSe	2.8	1.3×10^{16}	182
CdSe(STA)	2.5	1.5×10^{16}	148.8
Sb_2S_3	5.3×10^6	1.2×10^{12}	9.8
Sb_2S_3(STA)	5.0×10^6	2.4×10^{12}	9.2

Fig. 1. Variation in $(\alpha h\nu)^{1/2}$ vs. $(h\nu)$ for a typical film on ITO-coated glass substrate: (a) Sb_2S_3 film prepared with $10^{-5}M$ STA and annealed at 300°C in an N_2 atmosphere for 1 h, (b) same as (a) but without STA.
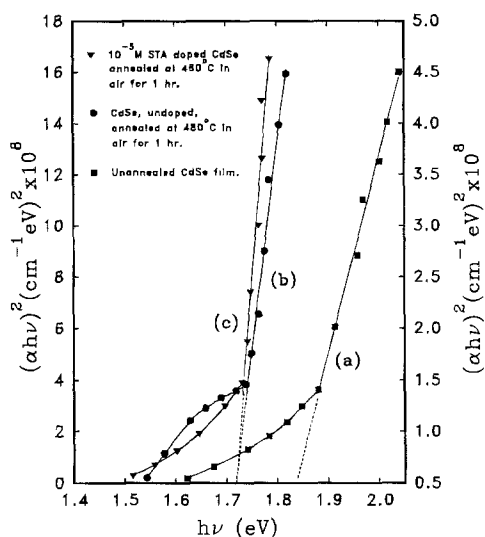

Fig. 2. Variation in $(\alpha h\nu)^2$ vs. $(h\nu)$ for a typical film on ITO-coated glass substrate: (a) as-deposited CdSe films, (b) same as (a) but annealed at 430°C in air for 1 h, and (c) same as (b) but the CdSe film is prepared with $10^{-5}M$ STA.

Good rectifications are also observed for both curves in the dark. Analogous behavior was obtained with Ni/CdSe, Ni/CdSe(STA), Au/CdSe, and Au/CdSe(STA) diodes. The saturation current density (J_0) and the ideality factor deduced from the dark ln (J)-V characteristics (forward bias) at 300 K for these different junctions are shown in Table II. The results shown in Fig. 3 and Table II indicate a significant decrease in n and J_0 for junctions fabricated with deposited films with STA. For comparison, the forward ln (J)-V characteristics of Pt/Sb_2S_3 and Pt/Sb_2S_3(STA) are presented in Fig. 4. Good rectification is observed for both curves in the dark. From these curves, the ideality factor (n) was found to be 1.78 for the Pt/Sb_2S_3 diode and 1.04 for the Pt/Sb_2S_3(STA) junction, whereas the saturation-current densities were 2.1×10^{-7} A · cm^{-3} and 1.5×10^{-9} A · cm^{-2} respectively. Similar trends were observed with the Ni/Sb_2S_3, Ni/Sb_2S_3(STA), Pt/Sb_2S_3, and Pt/Sb_2S_3(STA) diodes. The different values of J_0 and n deduced from the dark ln J-V characteristics (forward bias) at 300 K for these different junctions are shown in Table III. A significant decrease in n and J_0 occurred for the junctions fabricated with STA. Probably, the formation of a WO_3 interfacial layer, as con-
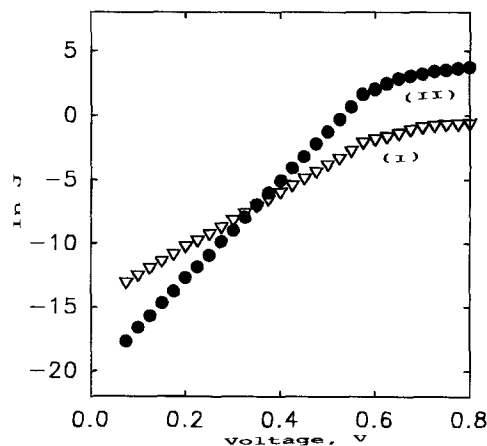

Fig. 3. Dark ln J-V characteristics (forward bias) at 300 K for Pt/n-CdSe: (I) for the CdSe films deposited without STA: barrier height $(\phi_b) = 0.59$ eV, $J_0 = 3.8 \times 10^{-7}$ A/cm^2, and ideality factor $(n) = 1.84$, and (II) for the CdSe films deposited with STA: barrier height $(\phi_b) = 0.81$ eV, $J_0 = 1.3 \times 10^{-9}$ A/cm^2, and ideality factor $(n) = 1.04$.

firmed by XPS and NAA [26-30] analysis, plays an important role in the electronic charge-transfer in the device and leads to the improvement in n and J_0. Figure 5(I) and (II) show the I-V characteristics of the Pt/CdSe and Pt/CdSe(STA) solar cells, under AM1 tungsten-halogen illumination from a series of these devices. The solar cell parameters obtained were: (I) for Pt/CdSe, $J_{sc} = 5.04$ mA/cm^2, $V_{oc} = 0.54$ V, $FF = 0.51$, giving the efficiency (η) of 1.4%, and (II) for Pt/CdSe(STA), $J_{sc} = 14.2$ mA/cm^2, $V_{oc} = 0.72$ V, $FF = 0.70$, showing an efficiency of 7.2%. The I-V characteristics for the Pt/Sb_2S_3 and Pt/Sb_2S_3(STA) Schottky barriers are presented in Fig. 6(I) and (II). The best solar cell parameters obtained from a series of these devices were: (I) for Pt/Sb_2S_3, $J_{sc} = 3.6$ mA/cm^2, $V_{oc} = 0.52$ V, $FF = 0.38$, giving an efficiency (η) of 0.7%, and (II) for Pt/Sb_2S_3(STA), $J_{sc} = 11.3$ mA/cm^2, $V_{oc} = 0.77$ V, $FF = 0.63$ with $\eta = 5.5\%$. The I-V characteristics of other metal/CdSe (with and without STA) and metal/Sb_2S_3 (with and without STA) Schottky diodes were also determined under AM1 illumination, and the deduced solar cell parameters are summarized in Table IV. As may be seen, all the devices fabricated with the films prepared with STA have improved solar cell parameters far more than those devices made with semiconductor films chemicaly deposited without STA. The variations in J_{sc}, η, and V_{oc} with the metal work functions (W) are shown in Fig. 7, 8, and 9, and the PV properties in Table IV for the devices fabricated with CdSe and Sb_2S_3 films chemically deposited with and without STA. A regular variation of η with W is observed for diodes fabricated with the films deposited with STA, whereas V_{oc} is observed to be independent of W (Fig. 9). The significant improvement in cell efficiency may be attributed to the favorable interface states introduced in the forbidden gap of the semiconductors used during the fabrication of these devices. These states may arise from the introduction of WO_3 (triclinic) in the films and may create localized states within the bandgap of WO_3. These states may be attributed to the states at energy levels within the bandgap and are responsible for the optical transitions. A study is now under way to help understand the charge-transfer processes between the polycrystalline grains of WO_3 and CdSe or

Table II. Ideality factor (n) and saturation current density (J_0) deduced from ln J-V characteristics (forward bias) at 300 K for different metal/CdSe Schottky junctions.

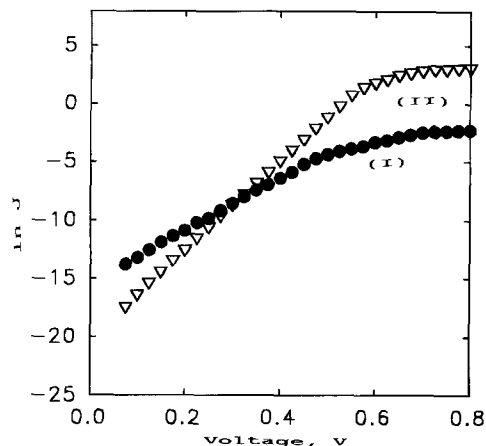| Junction	n	J_0 (A/cm^2)
Ni/CdSe	2.21	6.2×10^{-7}
Ni/CdSe(STA)	1.28	6.4×10^{-9}
Au/CdSe	2.04	4.2×10^{-7}
Au/CdSe(STA)	1.12	1.7×10^{-9}

Fig. 4. Dark ln J-V characteristics (forward bias) at 300 K for Pt/n-Sb$_2$S$_2$: (I) for the n-Sb$_2$S$_3$ films deposited without STA: barrier height (ϕ_b) = 0.63 eV, J_0 = 2.1 × 10^{-7} A/cm^2, and ideality factor (n) = 1.78, and (II) for the n-Sb$_2$S$_3$ films deposited with STA: barrier height (ϕ_b) = 0.81 eV, J_0 = 1.8 × 10^{-9} A/cm^2, and ideality factor (n) = 1.06.
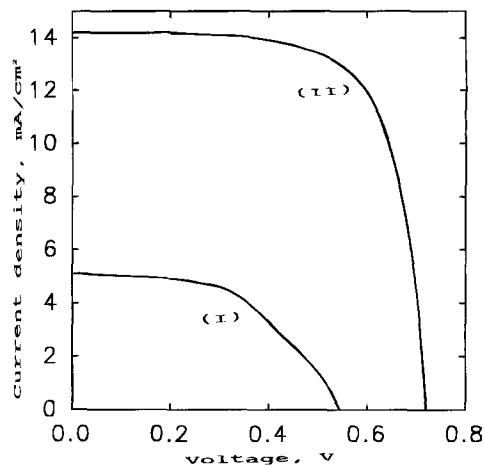

Fig. 5. Illuminated I-V characteristics of Pt/n-CdSe Schottky devices: (I) for the CdSe films deposited without STA: V_{oc} = 0.72 V, J_{sc} = 14.2 mA/cm^2, FF = 70.3%, and efficiency (η) = 7.2% and (II) for CdSe films deposited with STA: V_{oc} = 0.54 V, J_{sc} = 5.04 mA/cm^2, FF = 51%, and efficiency (η) = 1.4%.

Sb$_2$S$_3$. In particular, the transition energies due to the introduction of these states are actively being determined using electroluminescence and photoluminescence methods. Moreover, some assumptions may be derived from the band diagram scheme of Schottky diodes, including n-WO$_3$. From Fig. 10 it is clear that the conduction band of n-CdSe is higher than that of WO$_3$ and the Fermi level of Ni, Au, and Pt, respectively. The valence band of WO$_3$ lies below that of n-CdSe and the Fermi level of Ni, Au, and Pt, respectively. The same energy diagram is obtained for the Sb$_2$S$_3$/WO$_3$ heterojunction and the Ni, Au, and Pt Fermi levels. However, a hole in the valence band of the substrate (CdSe and Sb$_2$S$_3$) cannot travel downhill to the WO$_3$ valence band. It might be possible for hole transfer to occur through an intermediate energy level (e.g., interface states) located in the bandgap region of WO$_3$ when the electrodes are in contact with a metal. Accordingly, if the energy level of the metal is deeper in the energy scale and close to the valence band of WO$_3$, then the charge-transfer occurs more easily at the junctions. Furthermore, if the Fermi level of the metal used for the Schottky diodes is deeper in the energy scale, then the carriers of the interface states located in the WO$_3$ bandgap would be more important and would contribute to increasing the light absorption coefficient[32,33] (Fig. 1 and 2). Consequently, the beneficial effects of these states on the junction properties are observed in the improvement of the solar cell efficiencies (η) (Table IV), their ideality factor (n), and their dark current densities (J_0) (Fig. 3 and 4, Tables II and III) for diodes fabricated with the films deposited with STA. The decrease in the ideality factor from >2 for the junctions formed with the films deposited without STA to ~1 for those with films deposited with STA indicated a strong decrease in recombination processes due to the effect of these states. The optimization of the device parameters with the junction preparation conditions is under active investigation.

Fermi level pinning effect.—From Fig. 9, and Tables V and VI, no significant variation is observed in V_{oc} and W in a range of more than 1 eV for both types of diodes fabricated with the films deposited with and without STA. This
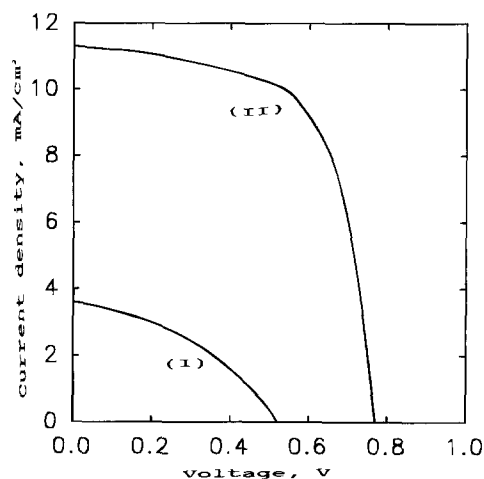

Fig. 6. Illuminated I-V characteristics of Pt/n-Sb$_2$S$_3$ Schottky devices: (I) for the Sb$_2$S$_3$ films deposited without STA: V_{oc} = 0.77 V, J_{sc} = 11.3 mA/cm^2, FF = 63%, and efficiency (η) = 5.5% and (II) for Sb$_2$S$_3$ films deposited with STA: V_{oc} = 0.52 V, J_{sc} = 3.6 mA/cm^2, FF = 38%, and efficiency (η) = 0.7%.

may indicate that the Fermi levels are pinned at these interfaces. Further support for this observation may be obtained by determining the barrier heights of these junctions. The C-V measurements (1 MHz) were carried out to determine the ϕ_b values. The 1/C^2-V plots for the Pt/CdSe, Pt/CdSe(STA), Pt/Sb$_2$S$_3$, and Pt/Sb$_2$S$_3$(STA) devices are shown in Fig. 11 and 12. The junctions formed with the n-CdSe and Sb$_2$S$_3$ films deposited with (STA) (Fig. 11(I)

Table III. Ideality factor (n) and saturation current density (J_0) deduced from ln J-V characteristics (forward bias) at 300 K for different metal/Sb$_2$S$_3$ Schottky junctions.

Junction	n	J_0 (A/cm^2)
Ni/Sb$_2$S$_3$	2.44	4.8 × 10^{-6}
Ni/Sb$_2$S$_3$(STA)	1.16	5.8 × 10^{-9}
Au/Sb$_2$S$_3$	2.32	3.2 × 10^{-6}
Au/Sb$_2$S$_3$(STA)	1.08	1.50 × 10^{-9}

Table IV. Solar cell parameters deduced from I-V characteristics under AM1 illumination for different metal/CdSe and metal/Sb$_2$S$_3$ junctions.

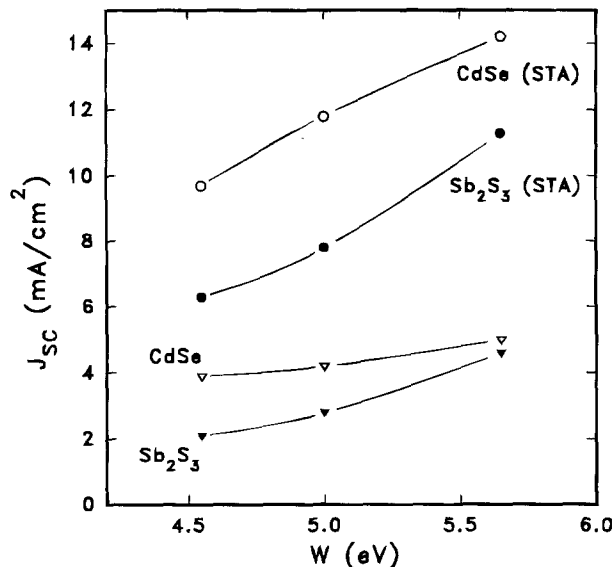| Junction	J_{sc} (mA/cm^2)	V_{oc} (V)	FF	η (%)
Ni/CdSe	3.90	0.49	0.42	0.80
Ni/CdSe(STA)	9.72	0.58	0.63	3.55
Ni/Sb$_2$S$_3$	2.24	0.44	0.31	0.3
Ni/Sb$_2$S$_3$(STA)	6.28	0.63	0.54	2.14
Au/CdSe	4.2	0.51	0.48	1.03
Au/CdSe(STA)	11.80	0.65	0.68	5.1
Au/Sb$_2$S$_3$	2.80	0.48	0.32	0.4
Au/Sb$_2$S$_3$(STA)	7.85	0.68	0.56	3.0
Pt/CdSe	5.04	0.54	0.51	1.4
Pt/CdSe(STA)	14.2	0.72	0.70	7.2
Pt/Sb$_3$S$_3$	3.6	0.52	0.38	0.7
Pt/Sb$_2$S$_3$(STA)	11.3	0.77	0.63	5.5

Fig. 7. Variations in J_{sc} with the metal work function (W): (○) for metal/n-CdSe(STA), (▽) for metal/n-CdSe, (●) for metal/n-Sb₂S₃(STA), and (▼) for metal/n-Sb₂S₃.
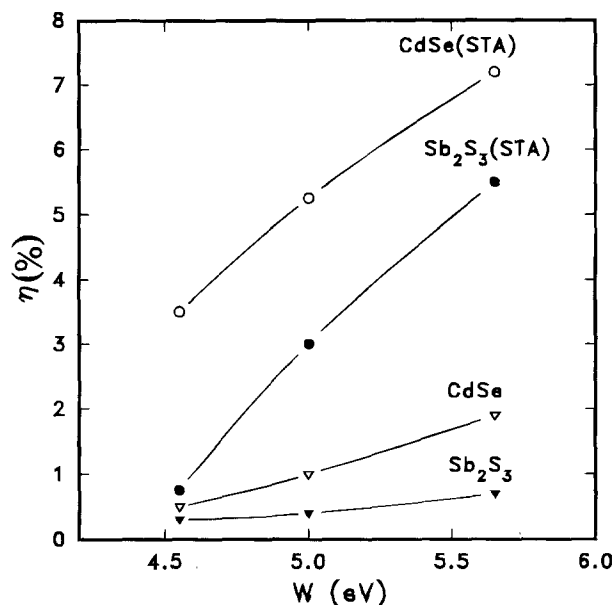
of metal/Sb_2S_3 (see Table VI). This indicates that the Fermi levels are pinned at the metal/CdSe, metal/CdSe(STA), metal/Sb_2S_3, and metal/Sb_2S_3(STA) diodes. Furthermore, the presence of Fermi level pinning on metal/CdSe(STA) and metal/Sb_2S_3(STA), in spite of the improvement in their ϕ_b or V_{oc}, indicates that the beneficial effects of the STA species in the films observed on metal/CdSe(STA) and metal/Sb_2S_3(STA) do not contribute to the suppression of the Fermi level pinning. It is interesting to note that this behavior is independent of the band structure of the semiconductor. Fermi level pinning is generally attributed to the presence of a high interface density, surface states[32-36] or carrier injection due to sufficient band-bending to change the relative carrier density.[37-42] It is interesting to note that for CdSe ($E_g = 1.70$ eV) and Sb_2S_3 ($E_g = 1.74$ eV) deposited without STA the Fermi levels are "pinned" at barrier heights very close to one-third (0.57 eV) of the bandgap from the valence-bandedge. These results are similar to those obtained on Si, GaAs, GaP,[42-44] and other semiconductors. Most covalent semiconductor surfaces having a high peak density, surface states, or defects show Fermi

Fig. 8. Variations in η with the metal work function (W): (○) for metal/n-CdSe(STA), (▽) for metal/n-CdSe, (●) for metal/n-Sb₂S₃(STA), and (▼) for metal/n-Sb₂S₃.
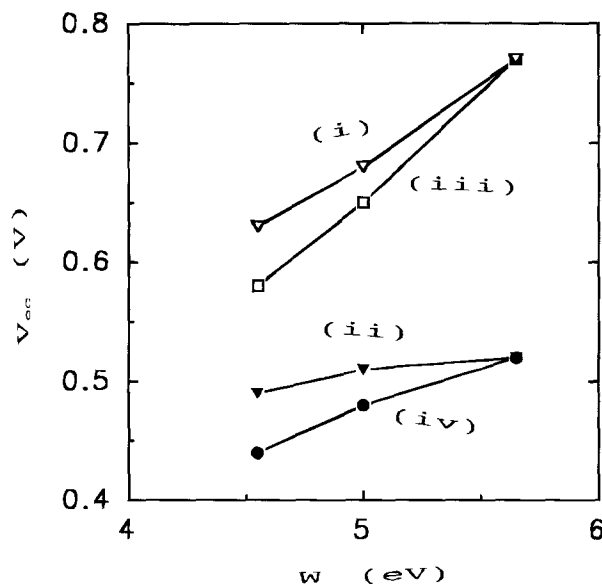
Fig. 9. Variations in V_{oc} with the metal work function (W): (△) for metal/n-CdSe(STA), (▼) for metal/n-CdSe, (○) for metal/n-Sb₂S₃(STA), and (●) for metal/n-Sb₂S₃.

and Fig. 12(I)) showed higher intercept voltages (V_i), 0.74 and 0.63 V, giving barrier heights (ϕ_b) of 0.83 and 0.81 eV, respectively, whereas the diodes fabricated with the n-CdSe and n-Sb_2S_3 films without STA showed a lower V_i, giving ϕ_b of 0.50 and 0.43 eV, respectively. From the slopes of the curves, the carrier concentrations were determined, and the values are summarized in Table I. Films deposited with STA have the same carrier concentrations as those deposited without STA. These values are consistent with the values determined by Hall measurements. The barrier heights are also in close agreement with those determined from the curves in Fig. 3 and 4. The ϕ_b values of the Schottky diodes on CdSe, CdSe(STA), Sb_2S_3, and Sb_2S_3(STA) are summarized in Table V and VI, respectively. The ϕ_b and V_{oc} values of metal/CdSe(STA) are ~200 mV greater than those of metal/CdSe diode. On the other hand, the barrier height of the metal/CdSe or the metal/CdSe(STA) diodes are practically independent of the metal work function (W) in a range of more than 1 eV. The same trend is observed if we compare the barrier heights of metal/Sb_2S_3(STA) to those

Fig. 10. n-CdSe/n-WO₃ or n-Sb₂S₃/n-WO₃ heterojunction band diagram.

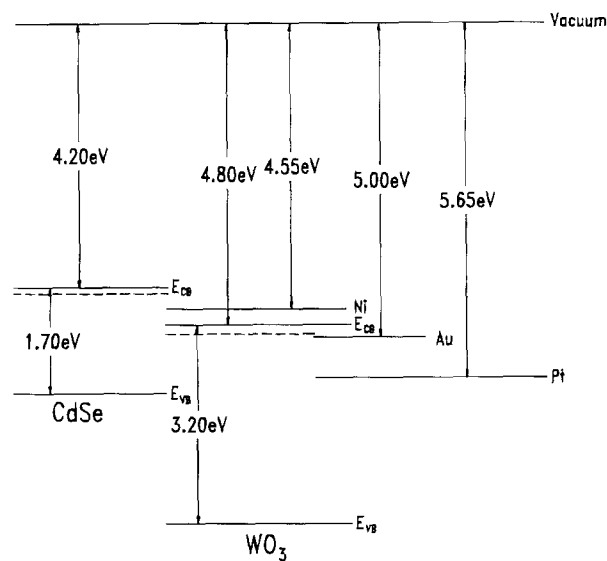**Table V. Variation in the barrier height (ϕ_b) deduced from C-V measurements and the open-circuit voltage (V_{oc}) of n-CdSe deposited with and without STA in contact with different metals.**

		Ni ($W = 4.55$ eV)	Au ($W = 5.00$ eV)	Pt ($W = 5.65$ eV)
ϕ_b (eV)	CdSe	0.53	0.57	0.62
	CdSe(STA)	0.74	0.81	0.83
V_{oc} (V)	CdSe	0.49	0.51	0.52
	CdSe(STA)	0.58	0.65	0.77

Table VI. Variation in the barrier height (ϕ_b) deduced from C-V measurements and the open-circuit voltage (V_{oc}) of n-Sb$_2$S$_3$ (with and without STA) in contact with different metals.

		Ni ($W = 4.55$ eV)	Au ($W = 5.00$ eV)	Pt ($W = 5.65$ eV)
ϕ_b (eV)	Sb$_2$S$_3$	0.53	0.57	0.63
	Sb$_2$S$_3$(STA)	0.75	0.74	0.79
V_{oc} (V)	Sb$_2$S$_3$	0.44	0.48	0.52
	Sb$_2$S$_3$(STA)	0.63	0.68	0.77

level pinning near one-third of the bandgap from the valence-bandedge. For CdSe and Sb$_2$S$_3$ films deposited with STA that have the same bandgap as the films deposited without STA,[26,27] the Fermi levels are "pinned" at a point slightly below the center of the forbidden gap (*e.g.*, 0.78 eV)
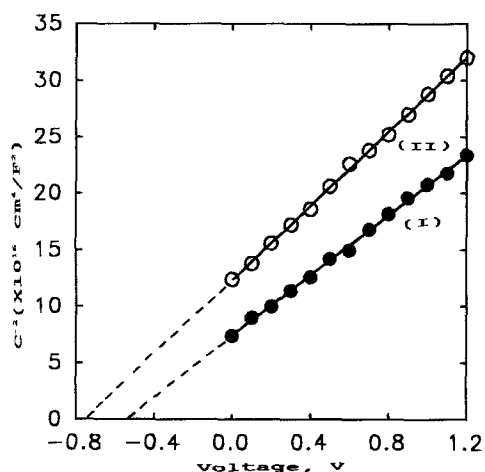

Fig. 11. 1/C^2 *vs.* V characteristics (reverse bias) at 300 K for Pt/n-CdSe Schottky devices: (I) for n-CdSe films deposited without STA, and (II) for n-CdSe films deposited with STA.
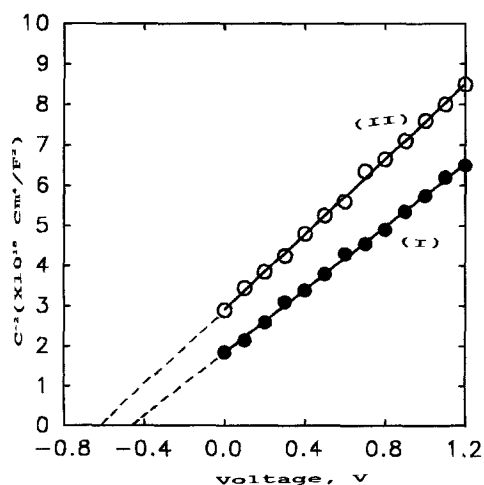

Fig. 12. 1/C^2 *vs.* V characteristics (reverse bias) at 300 K for Pt/n-Sb$_2$S$_3$ Schottky devices: (I) for n-Sb$_2$S$_3$ films deposited without STA, and (II) for n-Sb$_2$S$_3$ films deposited with STA.

of these semiconductors. Accordingly, these Fermi levels are pinned at a position different from that of films deposited without STA. This position of the "pinned" Fermi levels in the case of the films deposited with STA agrees well with that obtained by Pugh[45] from the theoretical calculations for <111> diamond, and it is observed that the Fermi level of diamond is pinned at a point slightly below the center of the forbidden gap. Our results on the films deposited with STA indicate evidence of the presence of a narrow band of surface or interface states slightly below the center of the forbidden gap of these two semiconductors.

Conclusion

The solar cell properties of Schottky diodes using the metals Pt, Au, and Ni on CdSe or Sb$_2$S$_3$ thin films chemically deposited with and without STA are reported. Based on the results obtained here, it may be concluded that:

1. A significant improvement in the Schottky barrier solar cell parameters was obtained with the CdSe or Sb$_2$S$_3$ films deposited with STA.

2. The improvement in solar cell properties was attributed to the presence of WO$_3$ in the films deposited with STA.

3. The absorption coefficient is improved due to the presence of WO$_3$ in the films.

4. The Fermi levels of the junctions fabricated with the CdSe or Sb$_2$S$_3$ films deposited with or without STA are pinned. For Schottky diodes fabricated with the CdSe or Sb$_2$S$_3$ films deposited without STA, the Fermi levels are pinned at one-third of the bandgap from the valence-bandedge. For junctions fabricated with CdSe or Sb$_2$S$_3$ deposited with STA, the Fermi levels are pinned at a point slightly below the center of the forbidden gap.

REFERENCES

1. S. A. Wessel and K. Kolbow, *Semicond. Sci. Technol.*, **2**, 747 (1987).
2. R. L. Van Meirhaeghe, R. van de Walle, W. H. Lafleche, and F. Cardon, *J. Appl. Phys.*, **70**, 2200 (1991).
3. J. Reichman and M. A. Russak, *ibid.*, **53**, 708 (1982).
4. K. C. Mandal and O. Savadogo, *J. Mater. Sci.*, **27**, 4355 (1992).
5. S. Licht and D. Peramunage, *Nature*, **345**, 330 (1990).
6. D. J. Arent, H. D. Rubin, Y. Chen, and A. B. Bocarsly, *This Journal*, **139**, 2705 (1992).
7. H. Sawatari and O. Oda, *J. Appl. Phys.*, **72**, 5004 (1992).
8. D. Cope, U.S. Pat. 2,875,359 (1959).
9. J. Grigas, J. Meshkauskas, and A. Orliukas, *Phys. Status Solidi A*, **37**, K39 (1976).
10. M. S. Ablova, A. A. Andreev, T. T. Dedegkaev, B. T. Melekh, A. B. Peutsov, N. S. Shendel, and L. N. Shumilova, *Soviet Phys. Semicond.*, **10**, 629 (1976).
11. M. J. Chockalingam, K. Nagarajo Rao, N. Ranjarajan, and C. V. Suryanarayana, *J. Phys., D*, **3**, 1641 (1970).
12. E. Montrimas and A. Pazera, *Thin Solid Films*, **34**, 65 (1976).
13. K. George and M. K. Radhakrishna, *Solid State Commun.*, **33**, 987 (1980).
14. A. Heller, K. C. Chang, and B. Miller, *This Journal*, **124**, 697 (1977).
15. A. B. Ellis, S. W. Kaiser, J. M. Bolts, and M. S. Wrighton, *J. Am. Chem. Soc.*, **99**, 2839 (1977).
16. S. Licht and D. Peramunage, *Nature*, **345**, 330 (1990).
17. R. C. Kainthla, D. K. Pandya, and K. L. Chopra, *This Journal*, **127**, 277 (1980).
18. D. M. Schleich, H. S. Chang, Y. I. Barberio, and K. J. Hanson, *ibid.*, **136**, 3274 (1989).
19. R. Lince, *J. Mater. Res.*, **5**, 218 (1990).

20. K. Saiki, K. Ueno, T. Shimada, and A. Kona, *J. Crystal Growth,* **95,** 603 (1989).
21. G. Hodes, J. Manassen, and D. Cahen, *ibid.,* **261,** 403 (1976).
22. M. A. Russak, J. Reichman, H. Witzke, S. K. Deb, and S. N. Chen, *This Journal,* **127,** 725 (1980).
23. G. Hodes, D. Cahen, J. Manassen, and M. David, *ibid.,* **127,** 2252 (1980).
24. C. J. Liu and J. H. Wang, *ibid.,* **129,** 719 (1982).
25. B. Miller, A. Heller, M. Robbins, S. Menezes, K. C. Chang, and J. Thomas, *ibid.,* **124,** 1019 (1977).
26. O. Savadogo and K. C. Mandal, *Mater. Chem. Phys.,* **31,** 301 (1992).
27. O. Savadogo and K. C. Mandal, *Solar Energy Mater. Solar Cells,* **26,** 117 (1992).
28. O. Savadogo and K. C. Mandal, *Electron. Lett.,* **28,** 1682 (1992).
29. O. Savadogo and K. C. Mandal, *Appl. Phys. Lett.,* **63,** 12 (1993).
30. O. Savadogo and K. C. Mandal, *J. Phys. D, Appl. Phys.,* **27,** 1070 (1994).
31. O. Savadogo and K. C. Mandal, *This Journal,* **139,** L16 (1992).
32. E. H. Rhoderick and R. H. Williams, *Metal-Semicon-*
ductor Contacts, 2nd ed., Clarendon Press, Oxford (1978).
33. A. Kireev, *Physique des semiconducteurs,* Mir, Moscou (1980).
34. O. Savadogo, *Can. J. Chem.,* **67,** 382 (1989).
35. A. J. Bard, A. B. Bocarsly, F. R. F. Fan, E. G. Walton, and M. S. Wrighton, *J. Am. Chem. Soc.,* **102,** 3671 (1980).
36. F. Schenmeyer and M.-S. Wrighton, *ibid.,* **102,** 6496 (1979).
37. O. Savadogo, J. Yazbeck, and A. Deschanvres, *Mater. Res. Bull.,* **18,** 1455 (1983).
38. F. R. Fan and A. J. Bard, *J. Am. Chem. Soc.,* **102,** 3677 (1980).
39. A. B. Bocarsly, D. C. Bookbinder, R. N. Dominey, N. S. Lewis, and M. S. Wrighton, *ibid.,* **102,** 3683 (1980).
40. J. Gobrecht, H. Gerischer, and H. Tributslh, *Ber. Bunseng. Phys. Chem.,* **82,** 1331 (1978).
41. J. A. Turner, J. Manassen, and A. J. Nozik, *Appl. Phys. Lett.,* **37,** 488 (1980).
42. R. N. Dominey, N. S. Lewis, and M. S. Wrighton, *J. Am. Chem. Soc.,* **103,** 1261 (1981).
43. S. M. Sze, in *Physics in Semiconductor Devices,* 2nd ed., p. 274, John Wiley & Sons, Inc., New York (1981).
44. C. A. Mead and W. C. Spitzer, *Phys. Rev.,* **134,** A713 (1964).
45. D. Pugh, *Phys. Rev. Lett.,* **12,** 390 (1964).

Electroluminescence and Photoluminescence of Cerium-Activated Alkaline Earth Thiogallate Thin Films and Devices

S-S. Sun* and R. T. Tuenge

Planar Systems, Incorporated, Beaverton, Oregon 97006

J. Kane and M. Ling

David Sarnoff Research Center, Princeton, New Jersey 08450

ABSTRACT

Thin films of cerium-activated alkaline earth thiogallate were investigated for the fabrication of blue-emitting thin-film electroluminescent (TFEL) devices. The films were prepared by RF sputtering from targets with composition: $M_{1-x}Ga_2S_4{:}Ce_x$, where M = Ba, Ca, Sr, and $0.01 \le x \le 0.1$. Photoluminescent (PL) emission spectra showed matching peak wavelengths to those obtained from electroluminescent (EL) emission for each alkaline earth thiogallate film. The optimum cerium concentration for EL emission intensity for strontium and calcium thiogallate films was determined to be $x = 0.04$ and 0.06, respectively. The EL brightness measured for the calcium thiogallate devices was almost twice that measured for the strontium thiogallate devices. This brightness variation, however, is due mainly to the difference in the lumen equivalent of the emission intensity. The cerium concentration dependence of the PL emission spectra of the thiogallate films is substantially decreased compared with the respective powder material suggesting inhomogeneous cerium incorporation in the films.

Blue-emitting EL phosphors have been actively investigated in recent years due to the importance of these materials for the development of full-color TFEL display panels. Insufficient luminance and color purity reported, respectively, for the known blue TFEL phosphors, ZnS:Tm and SrS:Ce, has led to a search for new electroluminescent phosphor host materials. Recently, cerium-activated alkaline earth thiogallates have been identified as bright blue electroluminescent emitters with sufficient color purity and stability to allow use in patterned phosphor full-color TFEL panels.[1] A luminance of 10 cd/m² at 60 Hz for a sputtered CaGa₂S₄:Ce TFEL device was reported in that first paper. This luminance level was adequate to use this phosphor as the blue component of an RGB (red, green, blue) patterned full-color VGA-size TFEL panel.

The CIE chromaticity coordinates of the blue TFEL emission measured for the cerium-doped calcium thiogal-

late phosphor are sufficient to produce a wide color gamut and a true white color when combined with EL red and green phosphors in a TFEL display panel. The related SrGa₂S₄:Ce phosphor achieved an even more saturated blue emission approaching that of the standard cathode ray tube (CRT) blue phosphor, but at the expense of lower brightness. The Ce doping concentration, coactivators, and processing conditions of the thiogallate films until now have not been reported and are expected to have an important effect on the luminescence and chromaticity of the thiogallate TFEL devices.

The cerium-activated alkaline earth thiogallates are efficient cathodoluminescent phosphors. Peters and Baglio[2] have reported cathodoluminescent (CL) spectra, CL efficiencies, and relative photoluminescence intensities for M²⁺Ga₂S₄:Ce,Na (M = Ca, Sr, and Ba) powders having a Ce³⁺ concentratom of 2 atomic percent (a/o). They did not, however, report on the cerium concentration dependence of the luminescence properties for these phosphors.

* Electrochemical Society Active Member.